Macromolecules **2003,** *36,* 359−367

Stress-Induced Reversible Phase Transition of Poly(tetramethylene naphthalate)

Kohji Tashiro,* Jue Cheng,[†] and Miyuki Ike

Department of Macromolecular Science, Graduate School of Science, Osaka University, Toyonaka, Osaka 560-0043, Japan, and College of Material Science and Engineering, Beijing University of Chemical Technology, Beisanhuan East Road, Beijing 100029, China

Received June 12, 2002; Revised Manuscript Received September 16, 2002

ABSTRACT: Crystalline modifications α and *β* of uniaxially oriented poly(tetramethylene naphthalate) [PTMN] sample have been found to show a reversible phase transition, which is induced by an application of a tensile force along the draw axis, as clarified by the measurement of polarized infrared spectra under tension. The transition behavior was found to be essentially the same with that observed for uniaxially oriented poly(tetramethylene terephthalte) [PTMT] sample. The *β* phase fraction, evaluated by quantitative analysis of the infrared spectra, was found to be linearly proportional to the strain and increase dramatically beyond a critical stress. The stress−strain curve measured for the bulk PTMN sample showed a plateau region, in which the α−*β* transition occurred. The plateau length became longer by raising the temperature of heat treatment of the samples or with increasing the degree of crystallinity. All these characteristic features are similar to those observed for PTMT. But, in the PTMT case, the plateau stress was almost constant irrespective of the annealing temperature. The stress−strain curve of the PTMT sample could be interpreted reasonably on the basis of a mechanical model in which α crystal and amorphous region are connected in a series mode. On the other hand, the plateau region in the stress−strain curve of the PTMN sample was found to shift apparently toward higher stress side and became more difficult to detect for the sample annealed at lower temperature. This was due to higher residual strain or *β* fraction remained in the sample. High-temperature annealing accelerated a stress relaxation, causing a recovery of the original α form and making the plateau part clearer. All these behaviors could be interpreted reasonably by employing a mechanical model in which a serially connected part of α crystal and amorphous region is combined in a parallel mode with a serial part of *β* crystal and amorphous region. The contribution of the *β* crystal is higher for the sample prepared at a lower temperature.

Introduction

Some of crystalline polymers exhibit various kinds of crystal modification depending on the sample preparation condition. These crystal modifications may show the phase transitions between them under a proper external field. One example can be seen for the phase transition induced by an application of external force along the chain axis.[1] Most of these transitions are irreversible and the crystal form obtained after transition does not return to the original crystal form even when the stress is relaxed. In such a sense, the phase transition observed for uniaxially oriented poly(tetramethylene terephthalate) [PTMT] is somewhat special because it occurs reversibly between α and *β* forms by increasing or decreasing stress.[2−20] The α form takes the molecular conformation including gauche-type C−C bonds (G) and the chain is slightly contracted, while the *β* form takes the fully extended conformation of the trans type (see Figure 1), where G and T are not exactly 60° and 180°, respectively.

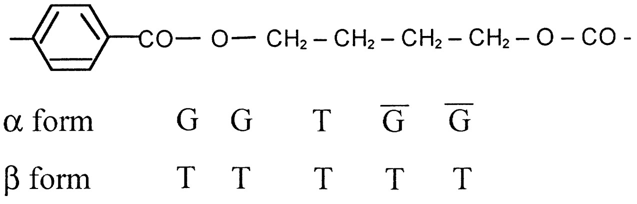

A similar type of reversible transition is observed also for several polymers such as poly(ethylene oxide),[21,22] poly(oxacyclobutane),[23] poly(3,3-dimethyl cyclobutane),[24] poly(tetramethylene succinate),[25] poly(trimethylene trephthalate),[26] etc. For example, in the case of poly(ethylene oxide), the transition occurs between TTG helical conformation and all-trans planar-zigzag conformation, although the transition is not perfect but occurs only partly before a breakdown of the sample.[21,22] These polymers are unique in such a common point that the stress−strain curve measured for the uniaxially oriented bulk sample shows a plateau of constant stress in a certain range of strain. This type of plateau is observed also for Keratin[27] and natural rubber.[28] All these phenomena could be interpreted reasonably in terms of the thermodynamic first-order phase transition.[13,25,27,28] Another characteristic point typically observed for the uniaxially oriented PTMT sample is that the plateau length is longer for the sample annealed at higher temperature or for the sample with a higher degree of crystallinity.[13] These observations could be interpreted quantitatively on the basis of a mechanical model constructed by a serial connection of crystalline α phase and amorphous region.[13,16] As the stress is increased, the α phase region experiences the transition to the *β* phase and the strain of the sample increases remarkably due to the increment of the crystallite size along the chain axis, giving a plateau in the stress−strain curve. Therefore it may be easily understood that the plateau length is proportional to the degree of crystallinity. At a terminal point of the plateau, the transition ceases and a slope of the stress−strain curve becomes steeper because the deformation of the *β* phase is started. In this way, the microscopically occurring

---

[†] College of Material Science and Engineering.

10.1021/ma020917d CCC: $25.00

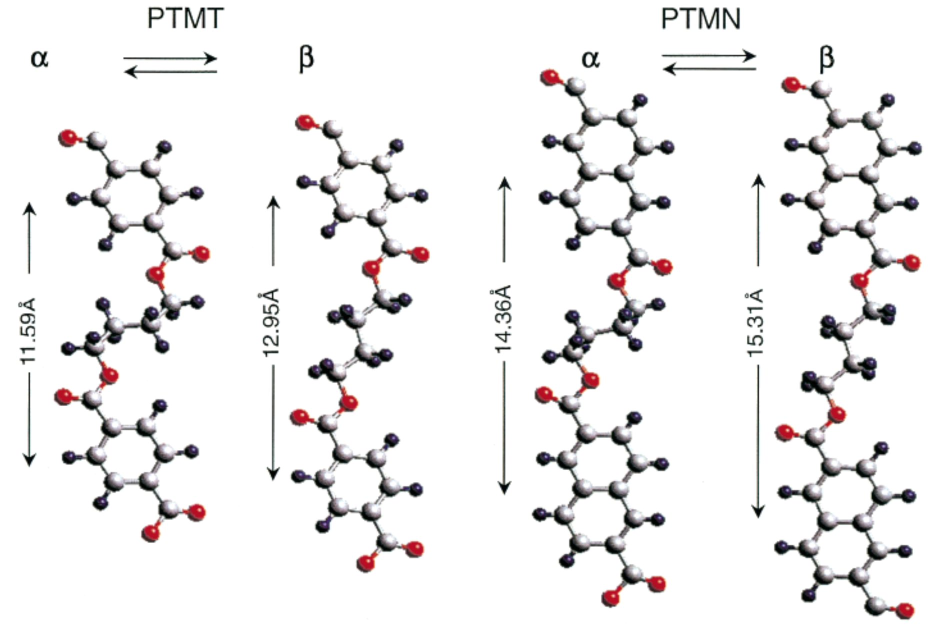

Figure 1. Molecular conformations of the α and β forms of poly(tetramethylene terephthalate)[5-8] and poly(tetramethylene naphthalate).[30]

α–β phase transition reflects explicitly on the stress–strain curve of the bulk sample.

Poly(tetramethylene naphthalate) [PTMN] has a chemical structure similar to that of PTMT and is expected to show similar type of polymorphism. In fact, PTMN is known to show the two kinds of crystal modification, α and β forms, as seen in Figure 1.[29,30] (The conformation of the β form is described here approximately as the all trans type, although the X-ray analysis reported the TST$\overline{\text{S}}$T conformation where S is skew.[30]) The α form of PTMN is obtained by slowly cooling the melt to room temperature. The oriented α form is prepared by stretching the melt-quenched sample at high-temperature close to the melting point (ca. 244 °C).[29,31,32] The β form is prepared by stretching the melt-quenched sample at relatively lower temperature.[29,33,34] By annealing this β form at high temperature, the α form is partially obtained. In the papers reported so far, however, nobody checked the possibility of a reversible phase transition occurring between the α and β forms, which might be induced by an application of tensile force as likely in the case of the PTMT sample.

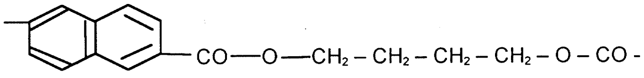

α form G G T $\overline{\text{G}}$ $\overline{\text{G}}$

β form T T T T T

In the present study, the reversible phase transition could be detected successfully for the first time for a uniaxially oriented PTMN sample through the infrared spectral measurement under tension. The transition behavior was found to be essentially the same as that observed for PTMT. A plateau region could be observed in the stress–strain curve, where the phase transition occurred. This stress–strain curve was interpreted reasonably on the basis of a mechanical complex model and compared with that proposed for PTMT sample.

Experimental Section

Samples. PTMN samples were kindly supplied by Teijin Co. Ltd., Japan. Since the molecular weight of the original sample was relatively low, the sample could not be stretched to enough high draw ratio. Therefore the samples were heated overnight at 200 °C below the melting point to increase the molecular weight through the solid-state polymerization reaction. The thus obtained samples could be stretched to about 4 times the original length at 100 °C, followed by heat treatment at the various temperatures of 100–220 °C for 2 h under tension. The thickness of the films used for infrared measurement was about 20 μm. For the measurement of X-ray fiber diagram, the rod samples were prepared in a similar way.

Measurements. Polarized infrared spectra were measured at room temperature for the uniaxially oriented films. The sample was set to a stretching device shown in Figure 2a and tensioned along the draw direction at a constant strain increment. In this measurement, the stress relaxation was considered to occur and so the infrared spectra were measured at a time when an almost constant stress was thought to have been reached. The infrared spectral measurement under a constant stress was also made, where the sample was set to the stretching device shown in Figure 2b. A small weight was applied, which was enlarged by several times at a sample position by utilizing a set of pulleys. The force on the sample was measured directly by a load cell. The infrared spectra were measured with a BioRad FTS60A/896 Fourier transform infrared spectrometer with a resolution power 2 cm^{-1}.

To check the crystal modifications in the samples, the X-ray fiber diagrams were taken before the infrared spectral measurements. A graphite-monochromatized Cu Kα line from a rotating-anode-type X-ray generator (MAC Science M18XHF) was irradiated to the sample, and the diffraction pattern was recorded by an imaging plate detector (DIP 1000 system, MAC Science).

Stress–strain curves were measured at room temperature by an Instron at a stretching rate of 4 mm/min (ca. 20% strain/min). Stress–strain curves were measured also by hanging a uniaxially oriented sample vertically, applying a weight, and reading out the change in sample length directly with a casettmeter. The stress–strain curves obtained by these two methods were essentially the same.

Results and Discussion

Infrared Spectral Changes under Tension. (A) Constant Strain Experiment. Figure 3 shows the

(a) Constant Strain

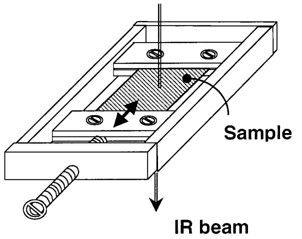

(b) Constant Stress

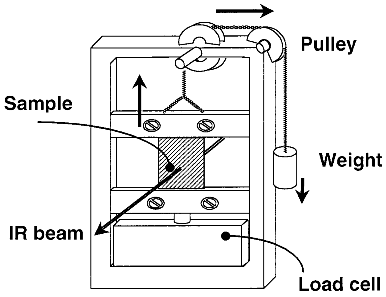

Figure 2. Illustrations of tensile machines used for the infrared spectral measurement under (a) constant strain and (b) constant stress.

strain dependence of the polarized infrared spectra measured for a uniaxially oriented PTMN sample annealed at 200 °C at stepwisely increased strains. Figure 4 shows the infrared spectra taken in the process of decreasing strain. At the starting point of the spectral measurement, the sample was almost of the α form, as checked by X-ray diffraction pattern. As the tensile strain was increased, the bands characteristic of the α form decreased in intensity and the bands of the *β* form increased instead. When the sample was relaxed (Figure 4), then the *β* bands decreased in intensity and the α bands increased again. But the recovery of the sample length was not perfect but stopped at ca. 4% strain. Therefore the infrared bands of both the α and *β* bands could be detected at this final stage of relaxation. This is due to the so-called residual strain. By heating this sample above the glass transition temperature (48 °C), the residual strain became smaller and the α bands increased in intensity furthermore. Figure 5 shows the strain dependence of the X-ray diffraction profile traced from the fiber diagrams measured for uniaxially oriented PTMN sample annealed at 220 °C. In a similar way to the infrared spectral change, the reflections intrinsic of the α form decreased in intensity and the reflection intensity of the *β* form increased with increasing tensile strain. All these phenomena observed in the infrared and X-ray diffraction measurements are quite similar to those reported for PTMT sample,[13] indicating clearly the existence of reversible solid-state phase transition between the α and *β* forms which is induced by tension and relaxation of the oriented sample along the chain direction.

The polarized infrared spectra of almost pure α and *β* forms are reproduced in Figure 6. Several bands characteristic of the α and *β* forms can be picked up. In the present paper we need only the identification of the infrared bands characteristic of the α and *β* phases. But, to know the microscopically viewed transition mechanism on the basis of these vibrational spectroscopic data, we may need to clarify the origin of these bands or the normal mode assignments. The detailed assignment of these bands is now being made on the basis of normal modes calculation.

(B) Quantitative Analysis of Infrared Spectra. On the basis of the infrared spectra given in Figures 3 and 4, the molar fractions of the α and *β* forms were estimated from the peak intensities of the bands. In this estimation a separation of the spectral profile into components was not made because the profile was too complicated to give a unique solution. Besides the contribution of the amorphous band component to the spectra was ignored as an approximation. To avoid some error coming from such an approximation, therefore, we chose the so-called crystallinity-sensitive bands with a high degree of infrared polarization character to estimate the change in the crystalline region as exactly as possible. Although the α and *β* fractions thus estimated might be only qualitative, they are good enough for the discussion of the transition mechanism as given below.

Let us assume that the phase transition occurs only between the α and *β* forms and no other intermediate form participates in this transition. This assumption can be checked by observing isobestic points (not shown here), which are the common points crossing many different spectral curves. The infrared absorbance $D_{\rm i}$ and the corresponding molar fraction $X_{\rm i}$ of the form i are expressed by Lambert–Beer's law as below.

$$D_{\rm i} = \epsilon_{\rm i} d X_{\rm i} \tag{1}$$

where $\epsilon_{\rm i}$ is a molar absorptivity, *d* is a film thickness, and i = α or *β*. Since the two components coexist at a certain strain, then

$$X_\alpha + X_\beta = 1 \tag{2}$$

From eqs 1 and 2, we have

$$D_\beta = -(\epsilon_\beta/\epsilon_\alpha)D_\alpha + \epsilon_\beta d \tag{3}$$

Therefore a plot of D_β against D_α should give a straight line with a slope $-(\epsilon_\beta/\epsilon_\alpha)$. Here we assume that the sample thickness *d* is almost constant and the $\epsilon_{\rm i}$ does not change even under tension as long as the strain is small. Figure 7 shows a plot of the infrared absorbance of the *β* form (1486 cm^{-1}) against that of the α form (1318 cm^{-1}), where the absorbance *D* was estimated as a weighted average of the parallel ($D_{//}$) and perpendicular ($D_\perp$) polarization components shown in Figures 3 and 4; $D = (2D_\perp + D_{//})/3$. By using the slope estimated from the straight line in Figure 7, $X_{\rm i}$ can be calculated as follows.

$$X_\beta = k/(1 + k) \qquad \text{where} \qquad k = (D_\beta/D_\alpha)/(\epsilon_\beta/\epsilon_\alpha) \tag{4}$$

X_β is plotted against strain as shown in Figure 8a. The stress–strain curve of the film was measured as shown in Figure 8c, from which the strain was converted to the stress, and then the X_β was replotted against stress as shown in Figure 8b. More ideally, stress and strain should be measured directly during the infrared measurement. But, in the present experiment of constant strain, the direct evaluation of stress could not be made. As will be shown in a later section, however, the stress dependence of X_β in Figure 8b is essentially the same as that obtained in the constant stress experiment.

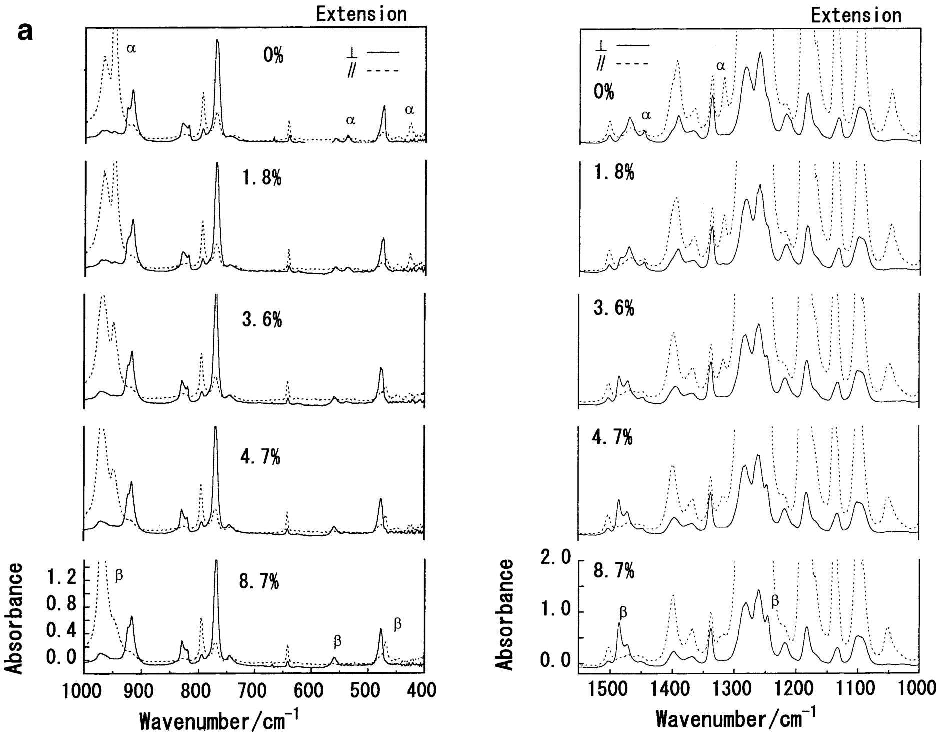

Figure 3. Strain dependence of polarized infrared spectra of oriented PTMN sample measured in the process of increasing strain. (a) Frequency region of 400–1000 cm^{-1} and (b) 1000–1600 cm^{-1}. - - -: Electric vector of incident infrared beam parallel to the draw axis. —: Electric vector of incident infrared beam perpendicular to the draw axis.

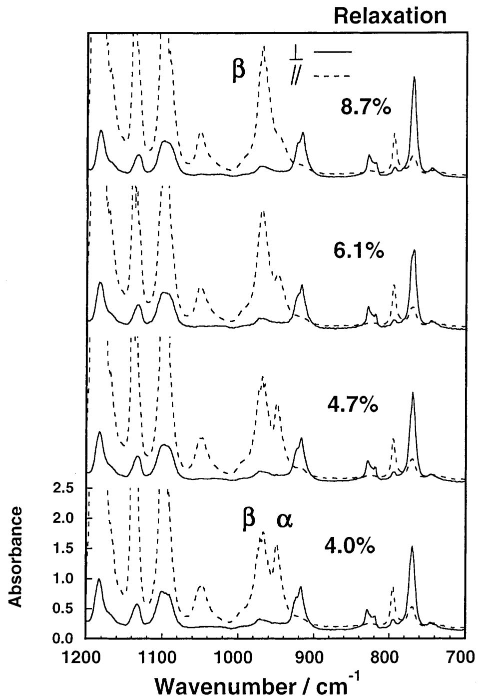

Figure 4. Strain dependence of polarized infrared spectra of oriented PTMN sample measured in the process of strain relaxation.

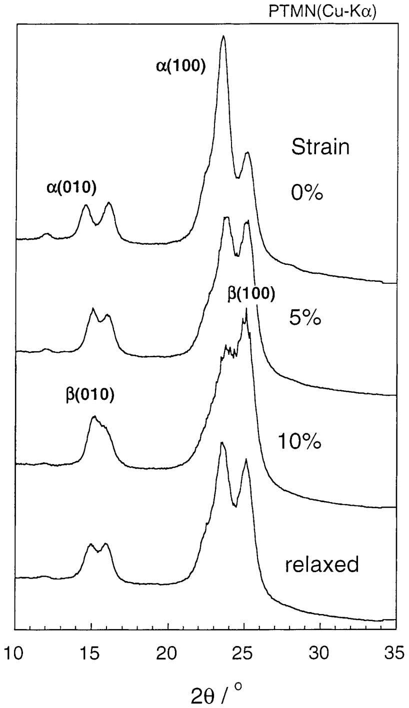

Figure 5. Strain dependence of equatorial X-ray diffraction profile measured for uniaxially oriented PTMN sample.

It is known from Figure 8a that X_β is almost linearly proportional to the strain in the range of 2–6%. This strain range is related with the starting and ending points of plateau region in Figure 8c. As seen in Figure 8b, the X_β is found to increases dramatically in the vicinity of a certain stress value, ca. 60 MPa, corresponding to the stress where the plateau is observed in Figure 8c. These phenomena are essentially the same as those observed for uniaxially sretched PTMT sample.[13] In the latter case, the phase transition between the α and β forms was interpreted reasonably in terms of the thermodynamic first-order transition. That is to say, when the Gibbs free energy is expressed as a function of stress, the free energies of the α and β phases cross at a critical stress σ^* and the phase transition from α to β phase occurs. The β phase is stable above σ^*. The transition of PTMN sample can be interpreted in a similar way.

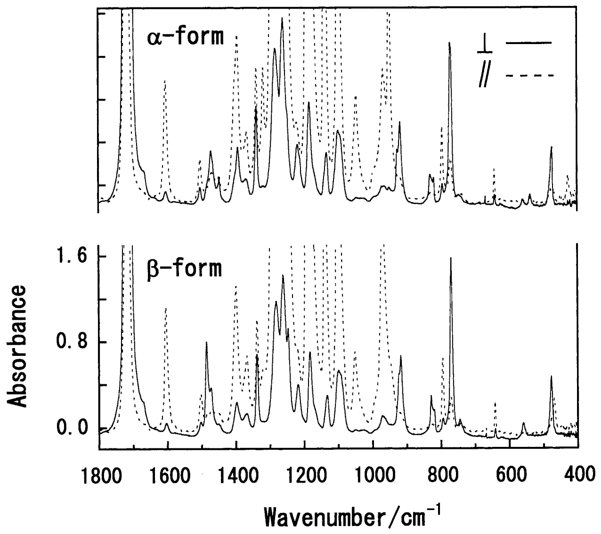

Figure 6. Polarized infrared spectra of α and β forms of PTMN. - -: Electric vector of incident infrared beam parallel to the draw axis, —: Electric vector of incident infrared beam perpendicular to the draw axis.

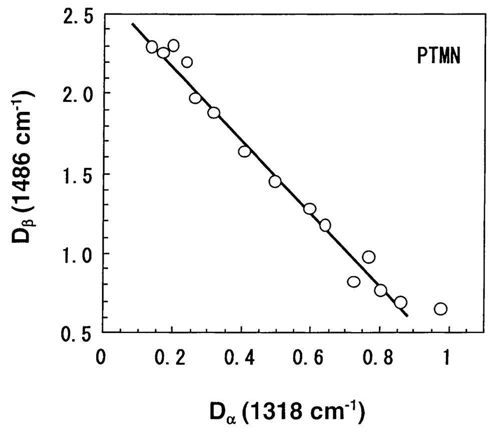

Figure 7. A plot of D_β against D_α, where D_i is an infrared absorbance of the i species (i = α and β forms).

When the sample was relaxed from the highest strain of ca. 8%, the X_β changed by following the X_β−strain curve observed in the extension process. However, X_β did not trace the X_β−stress curve observed in the extension process but remained at the value of $X_\beta = 0.5$ even after the sample was relaxed perfectly. Correspondingly, the stress−strain curve showed a large hysteresis and the residual strain of ca. 4% was detected even at the point of zero stress.

If the system is ideal the changes observed in Figure 8 should be sharper and the α−β transition should occur drastically at a certain stress value (see Figure 9a). However, in the actual system, the stress is considered to distribute heterogeneously among the various crystallites (Figure 9b). Therefore, even when the average stress of the bulk sample reaches σ^*, some of the crystallites may take the stress higher or lower than σ^*, giving a broader transition curve in a wider stress region (Figure 9c). In other words, the curve of Figure 8b is considered to be a convolution between the ideal X_β−stress curve (Figure 9a) and the distribution function of σ^* (Figure 9b).

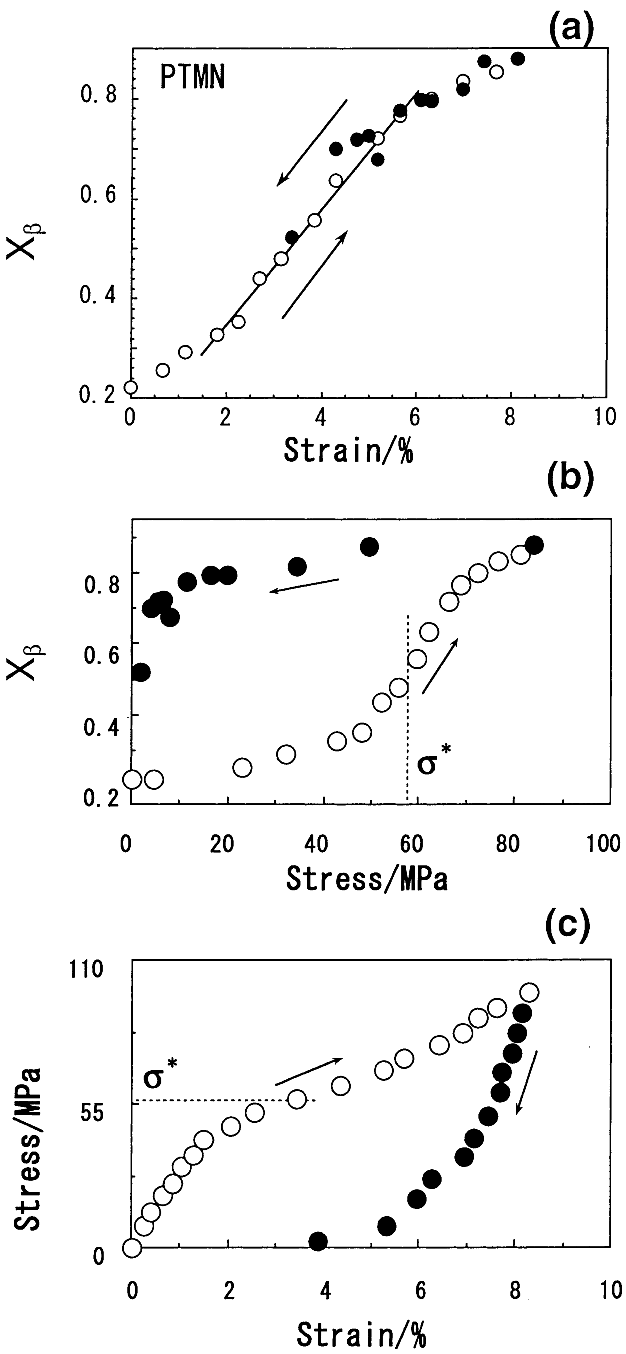

Figure 8. Dependence of molar fraction of the β form on (a) strain and (b) stress measured for the uniaxially oriented PTMN sample subjected to a tensile force. The stress was converted from the stress−strain curve shown in (c). Open and solid circles correspond to the processes of increasing and decreasing stress, respectively.

(C) Constant Stress Experiment. In the preceding section, the infrared spectral data measured under constant strain were analyzed. To obtain the X_β−stress curve shown in Figure 8b, the stress value was transferred from the separately measured stress−strain curve. However, due to the stress relaxation, we do not have any rational reason for this conversion between stress and strain. It is direct to measure the infrared spectra under constant stress and to compare the data with the X_β−stress relation shown in Figure 8b. The infrared spectra were measured by using an apparatus shown in Figure 2b. The measurement was made after the sample creep was considered to be almost saturated. The analytical procedure was the same as that mentioned above. In Figure 10 the thus-obtained X_β is plotted against the stress and the resulting curve is

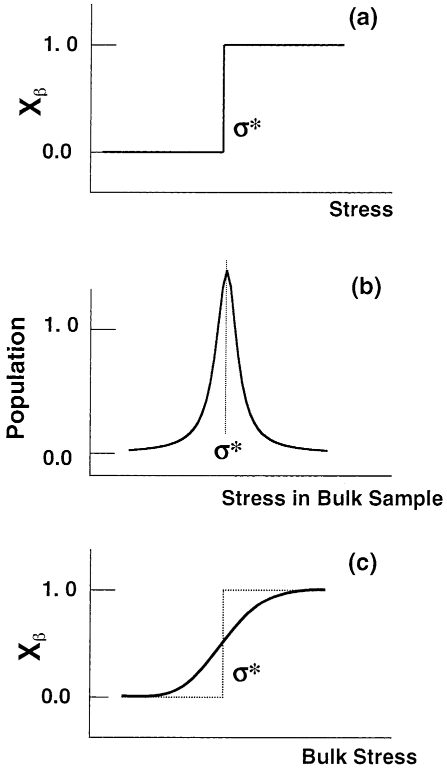

Figure 9. (a) Stress dependence of the molar fraction of β form in an ideal phase transition of PTMN crystal. The σ^* is a critical stress. (b) Distribution of stress in the bulk sample subjected to an average stress value σ^*. (c) Actually observed stress dependence of the β fraction. The curve is obtained as a convolution between the curves given in (a) and (b).

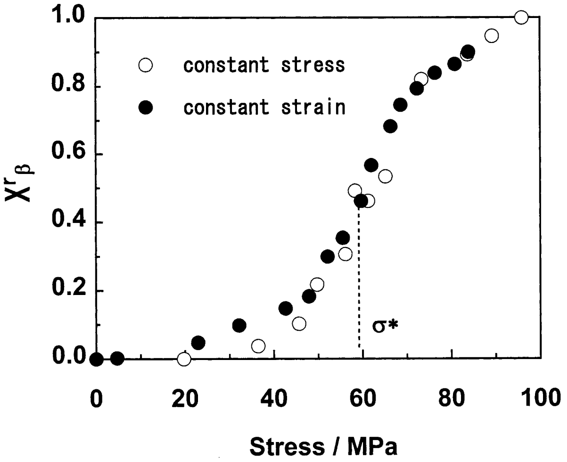

Figure 10. Stress dependence of the β molar fraction compared between the experiments made under constant stress (○) and constant strain (●) (refer to Figure 8b).

compared to the curve of Figure 8b. These two experimental data are essentially the same within the experimental error. Therefore it may be confirmed here that the X_β increases steeply in the narrow region of a certain stress, about 60 MPa, indicating the existence of a critical stress, as mentioned in the previous section.

Stress–Strain Curve and α–β Transition. The stress–strain curves were measured for the uniaxially oriented PTMN samples annealed at the various temperatures. The results are shown in Figure 11 in comparison with the stress–strain curves measured for the uniaxially oriented PTMT samples. In the case of the PTMT samples (Figure 11a), the stress in the plateau region is approximately constant and the plateau length is longer for the sample annealed at higher temperature.[13] In contrast, the plateau becomes more obscure for the PTMN sample annealed at lower temperature, the stress of which is apparently higher. This high contrast in the stress–strain curve between PTMT and PTMN may reflect a large difference in the stress distribution in the bulk sample.

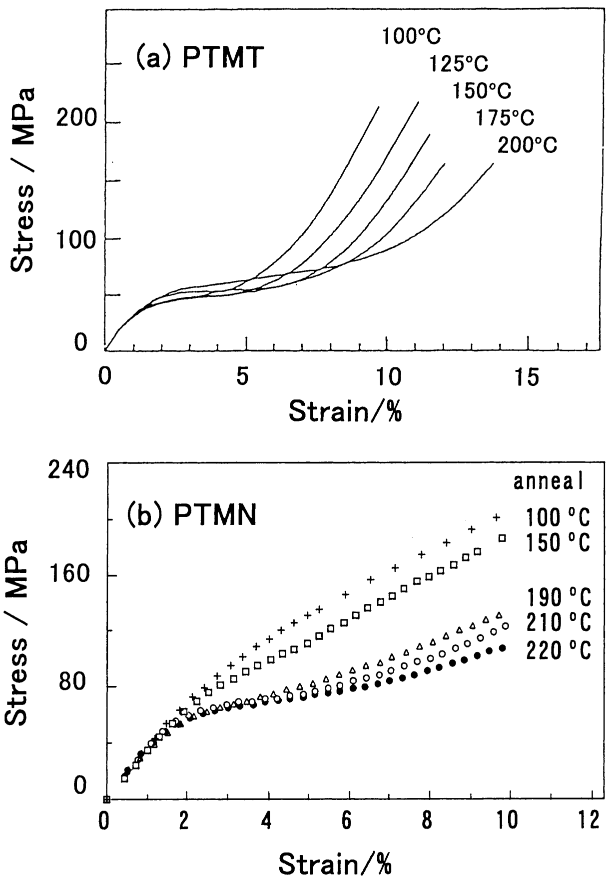

Figure 11. Stress–strain curves measured for uniaxially oriented (a) PTMT[13] and (b) PTMN samples annealed at various temperatures.

(A) Stress–Strain Curves of PTMT (Review). In the previous papers we discussed the changes in stress–strain curves of PTMT[13] and its multiblock copolymers with tetramethylene oxide segments.[16] It must be emphasized here that these stress–strain curves were measured for the samples which were prepared by uniaxially drawing the unoriented samples up to the natural draw ratio of ca. 4 times the original length after necking, followed by heat treatment at the various temperatures under tension. (The stress–strain curves are considered to be affected sensitively by the change in the sample preparation conditions. For example, an injection molded PTMT sample was reported to give double yield points before necking due to the deformation in the amorphous region and the phase transition in the crystalline region.[20]) The curves of the uniaxially oriented PTMT samples could be interpreted reasonably on the basis of a mechanical model consisting of crystalline and amorphous phases in a series mode, as illustrated in Figure 12. The crystalline region experiences a phase transition at a critical stress σ^*. Below σ^*, the α crystalline form is deformed elastically and gives a straight stress–strain curve. At σ^*, the phase transition occurs from α to β form and the crystallite

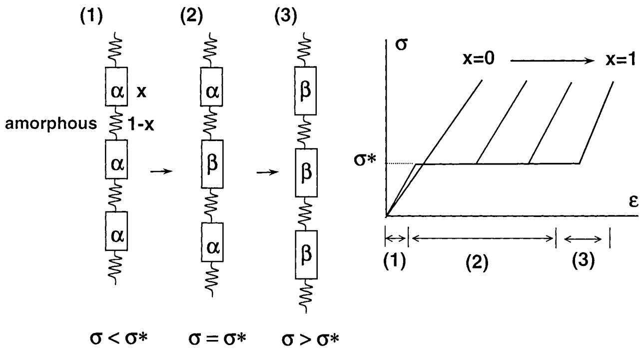

Figure 12. The mechanical model of uniaxially oriented PTMT sample and stress–strain curves predicted for the samples with various degrees of crystallinity.

length increases drastically by about 12%, the difference in the fiber period between these two forms. As a result the plateau is created in the stress–strain curve. Above σ* all the α crystallites transfer to the β form, which is deformed elastically and gives the straight stress–strain curve again. During this complicated change in the crystalline region, the amorphous phase is deformed elastically and gives the straight stress–strain line. Since these two phases are arranged in series, the plateau length of the stress–strain curve is longer for the sample with higher degree of crystallinity. The similar phenomenon is observed also for the multiblock copolymers of PTMT and poly(tetramethylene oxide).[16] In the case of elastomer, the amorphous region is very soft at room temperature compared with that of PTMT homopolymer, and therefore the whole stress–strain curve becomes almost flat in a wide strain region. But the plateau region can be still observed, because the phase transition from the α to β form occurs as detected by infrared spectral measurement under tension. At low temperature below the glass transition (−30 °C), the amorphous region is harder and the stress–strain curve changes to the curve similar to that of PTMT homopolymer, and the transition from the α form to the β form can be observed more clearly in a narrower strain region.

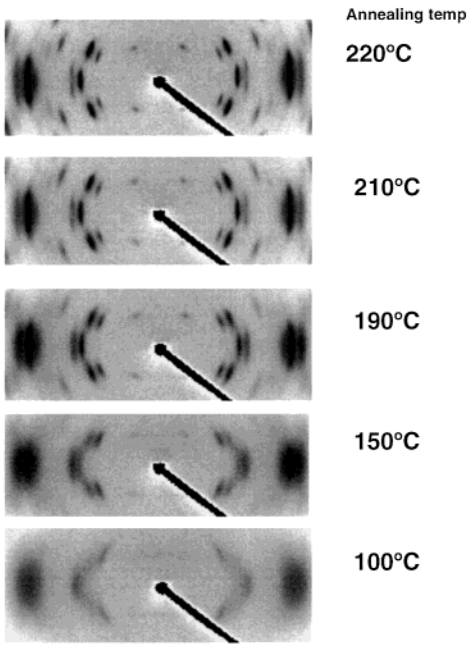

Figure 13. X-ray fiber diagrams taken for uniaxially oriented PTMN samples annealed at the various temperatures.

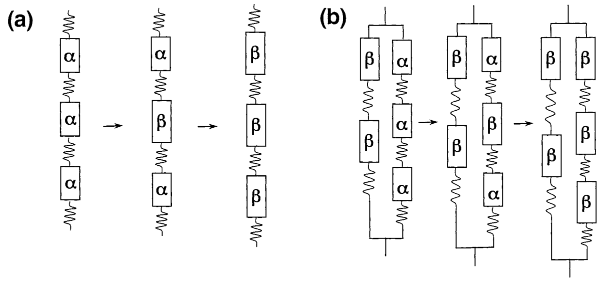

Figure 14. Comparison of mechanical model between (a) uniaxially oriented PTMT sample and (b) uniaxially oriented PTMN sample. By stretching, the α crystalline region changes into the β form, but the β form does not change at all.

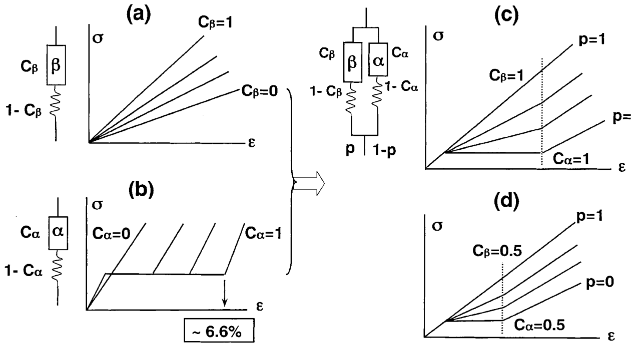

Figure 15. Mechanical model of uniaxially oriented PTMN sample with various degrees of crystallinity. (a) A serial component of the β crystalline phase and the amorphous region. (b) A serial component of the α crystalline phase and the amorphous region. (c) Parallel combination of components (a) and (b) and the stress–strain curves predicted for the samples with various *p* ratios. The crystallinity (Cα and Cβ) is assumed to be 100%. (d) The same parameters used in (c) used for the samples of 50% crystallinity.

(B) Stress–Strain Curves of PTMN. As pointed out before, the stress–strain curve of uniaxially oriented PTMN sample was different from the above-mentioned PTMT case. As detected by X-ray diffraction and infrared spectral measurements, the PTMN sample stretched at 100 °C and annealed at relatively low temperature exhibits a high amount of the β form although the degree of crystallinity is low (see Figure 13). When the sample is annealed at such a high temperature as 200 °C, the sample is rich of the α form due to the stress relaxation. As seen in Figure 11, the sample annealed at lower temperature or the sample with higher β content shows apparently the plateau part in higher stress region. From these situations, we may speculate that (i) the sample annealed at a certain temperature is a mixture of the α and β forms due to the residual strain, (ii) these α and β forms are in the mechanically parallel relation and the total stress is a summation of stress components working in these two regions, (iii) only the α region can experience the phase transition to the β form, and (iv) the β form does not show any transition. Figure 14 b illustrates this situation clearly in comparison with the bahvior of PTMT sample shown in Figure 14a. Figure 15 shows the stress strain curves predicted for the model given in Figure 14 b. Figure 15a shows the stress–strain curves of a serial combination of β form and amorphous region. The stress–strain curve, which is assumed to be a straight line, changes its slope depending on the β content. In Figure 15b, where the series model of α form and amorphous region is shown, the stress−strain curve exhibits a plateau region and its length changes depending on the α content. In the plateau region the α−β transition occurs and the end point of the plateau is about 6.6%, a difference in fiber period between the α and β forms.[30] By combining these two series models of Figure 15a,b in parallel at a ratio of p:1−p, we obtain total stress−strain curves. Figure 15c is for the case of pure crystal. The $p = 0$ gives the stress−strain curve of the pure α form with a long plateau. The ratio $p = 1$ is the case of pure β form. If the ratio p is changed from 0 to 1, then the stress−strain curve changes its shape between these two extreme cases. When the crystallinity (Cα and Cβ) is not 100%, the plateau region becomes shorter and is more difficult to detect although the essential shape of the stress−strain curve is kept unchanged.

The stress−strain curves predicted here are qualitatively in good agreement with the actually observed data given in Figure 11b. For the quantitative reproduction of the actually observed curves, we need to know the exact values of the Young's moduli intrinsic of the pure α and β forms and amorphous phase, the degrees of crystallinity (Cα and Cβ), and the ratio p between the two parallel components. It is now difficult to obtain the concrete values of these parameters experimentally.

(C) Comparison of Mechanical Properties between PTMT and PTMN. Here we have a question why the mechanical behavior is different between PTMT and PTMN samples. The reversible phase transition between the α and β forms is common to these two polymers. However, when the sample is relaxed from the β form, the return to the original α form is relatively easy for PTMT but it is difficult for PTMN. In other words, the residual strain is higher for PTMN than PTMT. This residual strain disappears by heating at high temperature under free tension. Therefore the stress relaxation is considered to relate with the thermal motion of molecular chains. The glass transition is 48 °C for PTMN, higher than that of PTMT (40 °C). Therefore the thermal mobility of chains at room temperature seems lower for PTMN than that for PTMT. Although this difference in thermal mobility might be small, higher residual strain at room temperature is considered to occur more remarkably in PTMN than PTMT.

Conclusions

In the present paper the reversible phase transition of uniaxially oriented PTMN sample was measured by X-ray diffraction and infrared spectroscopy under constant strain (or stress) condition. The β fraction, evaluated by quantitative analysis of the infrared spectra, was found to increase in proportion to the strain ($2 <$ strain $< 7\%$) and to increase remarkably in the vicinity of a critical stress (about 60 MPa). The stress−strain curve showed a plateau region, in which the α−β transition was observed. All these phenomena were found to be the same with those of PTMT sample, and could be interpreted in terms of thermodynamic first-order transition between the α and β forms.

The stress−strain curves of uniaxially oriented PTMN samples annealed at various temperatures were found to behave in a quite different manner from those of PTMT samples. In the latter case the stress−strain curve was essentially the same for any sample and only the plateau length changed depending on the degree of crystallinity. That is to say, the stress−strain curves can be interpreted reasonably on the basis of mechanical series model between the α crystal phase and the amorphous phase. On the other hand, the PTMN samples showed the stress−strain curves in which the plateau stress was apparently higher for the sample annealed at lower temperature or the sample with higher content of the β form. This curious behavior could be interpreted qualitatively by assuming a parallel combination of two types of series models, one consisting of the pure α form and amorphous phase and the other of the pure β form and amorphous phase. The latter component was needed due to the existence of residual strain in the sample.

In this way the crystalline phase transition itself is quite similar to each other between these two kinds of polyester, but the mechanical behavior of the bulk sample or the stress distribution in the sample is quite different between these two samples. To understand this difference, the aggregation structure of chains in the crystalline and amorphous regions is needed to compare between these two samples. The factors related with the stress relaxation such as the molecular motion, the chain flexibility, etc. might be also important in understanding the difference in the residual stress of the samples. Anyway, it is important to notice here that a change from benzene to naphthalene ring in the skeletal chain structure of PTMT does not give a large difference in the crystal structure and the corresponding phase transition behavior between PTMT and PTMN, but it causes a remarkable difference in the mechanical behavior of the bulk samples.

Acknowledgment. The authors thank Teijin Co. Ltd., Japan, for their kind supply of PTMN samples. They thank also Toyobo Research Center Co. Ltd., Japan, for giving them a chance to use an Instron machine. One of the authors (J.C.) thanks Beijing University of Chemical Technology for giving her a chance to carry out this research in Osaka University and the AIEJ (Association of International Education, Japan) Short-Term Student Exchange Promotion Program Scholarship for financial support during her stay in Osaka University. The authors thank Dr. Chellaswamy Ramesh of National Chemical Laboratory, India, for his kind advice in the performance of the experiment.

References and Notes

(1) Tashiro, K.; Tadokoro, K. *Encycolpedia of Polymer Science and Engineering, Supplement*, 2nd ed.; John-Wiley & Sons: New York, 1989; p 187.
(2) Biye, A.; Overton, J. R. *Bull. Am. Phys. Ser. 2* **1974**, *19*, 352.
(3) Jakeways, R.; Ward, I. M.; Wilding, M. A.; Hall, I. H.; Desborough, I. J.; Pass, M. G. *J. Polym. Sci., Polym. Phys. Ed.* **1975**, *13*, 799.
(4) Ward, I. M.; Wilding, M. A.; Brondy, H. *J. Polym. Sci., Polym. Phys. Ed.* **1976**, *14*, 263.
(5) Mencik, Z. *J. Polym. Sci., Polym. Phys. Ed.* **1975**, *13*, 2173.
(6) Yokouchi, M.; Sakakibara, Y.; Chatani, Y.; Tadokoro, H.; Tanaka, T.; Yoda, K. *Macromolecules* **1976**, *9*, 266.
(7) Alter, U.; Bonart, R. *Colloid Polym. Sci.* **1976**, *254*, 348.
(8) Desborough, I. J.; Hall, I. H. *Polymer* **1977**, *18*, 825.
(9) Stambaugh, B. D.; Koenig, J. L.; Lando, J. B. *J. Polym. Sci., Polym. Lett.* **1977**, *15*, 299.
(10) Stambaugh, B.; Koenig, J. L.; Lando, J. B. *J. Polym. Sci., Polym. Phys. Ed.* **1979**, *17*, 1053.
(11) Siesler, H. W. *Makromol. Chem.* **1979**, *180*, 2261.
(12) Stach, W.; Holland-Moritz, K. *J. Mol. Struct.* **1980**, *60*, 49.
(13) Tashiro, K.; Nakai, Y.; Kobayashi, M.; Tadokoro, H. *Macromolecules* **1980**, *13*, 137.
(14) Gillette, P. C.; Dirlikov, S. D.; Koenig, J. L.; Lando, J. B. *Polymer* **1982**, *23*, 1759.

(15) Gillette, P. C.; Lando, J. B.; Koenig, J. L. *Polymer* **1985**, *26*, 235.
(16) Tashiro, K.; Hitramatsu, M.; Ii, T.; Kobyashi, M.; Tadokoro, H. *Sen-i Gakkaishi* **1986**, *42*, T-597.
(17) Tashiro, K.; Hitramatsu, M.; Ii, T.; Kobyashi, M.; Tadokoro, H. *Sen-i Gakkaishi* **1986**, *42*, T-659.
(18) Dobrovolny-Marand, E.; Hsu, S. L.; Shih, C. K. *Macromolecules* **1987**, *20*, 1022.
(19) Grasso, R. P.; Perry, B. C.; Koenig, J. L.; Lando, J. B. *Macromolecules* **1989**, *22*, 1267.
(20) Muramatsu, S.; Lando, J. B. *Polym. Eng. Sci.* **1995**, *35*, 1077.
(21) Takahashi, Y.; Sumita, I.; Tadokoro, H. *J. Polym. Sci., Polym. Phys. Ed.* **1973**, *11*, 2113.
(22) Tashiro, K.; Tadokoro, H. *Rep. Prog. Polym. Phys. Jpn.* **1978**, *21*, 417.
(23) Takahashi, Y.; Osaki, Y.; Tadokoro, H. *J. Polym. Sci., Polym. Phys. Ed.* **1981**, *19*, 1153.
(24) Takahashi, Y.; Osaki, Y.; Tadokoro, H. *J. Polym. Sci., Polym. Phys. Ed.* **1980**, *18*, 1863.
(25) Ichikawa, Y.; Washiyama, J.; Moteki, Y.; Noguchi, K.; Okuyama, K. *Polym. J.* **1995**, *27*, 1230.
(26) Wu, J.; Schultz, J. M.; Samon, J. M.; Pangelinan, A. B.; Chuah, H. H. *Polymer* **2001**, *42*, 7141.
(27) Ciferri, A. *Trans. Faraday Soc.* **1963**, *59*, 562.
(28) Oth, J. F. M.; Flory, P. J. *J. Am. Chem. Soc.* **1958**, *80*, 1297.
(29) Watanabe, H. *Kobunshi Ronbunshu* **1976**, *33*, 229.
(30) Koyano, H.; Yamamoto, Y.; Saito, Y.; Yamanobe, T.; Komoto, T. *Polymer* **1998**, *39*, 4385.
(31) Yoon, K. H.; Lee, S. C.; Park, O. O. *Polym. J.* **1994**, *26*, 816.
(32) Lee, S. C.; Yoon, K. H.; Kim, J. H. *Polym. J.* **1997**, *29*, 1.
(33) Yamanobe, T.; Matsua, H.; Imai, K.; Hirata, A.; Mori, S.; Komoto, T. *Polym. J.* **1996**, *28*, 177.
(34) Chiba, T.; Asai, S.; Xu, W.; Sumita, M. *J. Polym. Sci.: Part B: Polym. Phys.* **1999**, *37*, 561.

MA020917D